Numerical simulation of internal (gravity) wave dynamics

Nils P. Wedi

ECMWF, Shinfield Park, Reading
RG2 9AX, United Kingdom
wedi@ecmwf.int

ABSTRACT

The direct numerical simulation (DNS) of the laboratory experiment of Plumb and McEwan (1978) exhibits wave reflection, wave interference, wave-mean flow interaction and wave breaking. It enables the study of internal (gravity) wave processes and their numerical realisability in a confined "laboratory" environment. Conclusions are drawn on the numerical realisability of equatorial mean flow oscillations in weather prediction and climate models, which are believed to be driven by internal wave processes.

1 Introduction

Internal (gravity) waves propagate in stably stratified atmospheres and oceans. The stratification results from the vertical temperature gradient or from concentration gradients such as the solution of salt in water. Internal waves reflect in many ways the more easily observed behaviour of surface water waves. For example, one observes the interference of waves originating from different sources, wave reflection at internal or external boundaries, wave-mean flow interactions, wave dissipation due to critical layer momentum fluxes, and the onset of turbulence due to wave breaking. This transition from wave instabilities to turbulence for internal gravity waves has been comprehensively reviewed in Staquet and Sommeria (2002). Atmospheric gravity wave dynamics have been reviewed in Fritts and Alexander (2003). Often, the individual wave processes are not always distinctively separable, and as will be shown, one of the above wave processes may be the cause of another, e.g. propagating gravity waves may themselves form subsequently "self-destructing" zonal mean flow layers (Grimshaw, 1975; Galmiche et al., 2000). Analytic or semi-analytic methods, based on the assumption of separability of horizontal and vertical motions, i.e. normal mode analysis, have been employed to obtain a principal wave guide of the atmosphere (Phillips, 1990; Daley, 1988; Kasahara and Qian, 2000; Thuburn et al., 2001) and references therein. The assumption of a scale separability between a "slowly-varying" background (mean) flow and propagating waves, called the WKB(J) approximation (Gill, 1982), has been used to explain the propagation of groups of waves in a "slowly-varying" (with respect to the individual wave oscillations) dissipative medium (Bretherton, 1966; Grimshaw, 1972, 1974, 1975). Using these methods, substantial progress has been made in the understanding of linear and nonlinear internal wave phenomena, e.g. (Booker and Bretherton, 1967; Phillips, 1981, 1990). These studies have been complemented by laboratory experiments, e.g. (Koop, 1981; Koop and McGee, 1986; Baines, 1995). However, especially, the interaction of waves with each other and with the background flow, and the inherent nonlinearity of wave breaking processes, make it difficult to deduce a complete understanding of internal wave dynamics from experimental evidence alone. Now, with the advance of modern computers and accurate numerical methods, direct numerical simulations (DNS) emerge as useful tools for explorations of fully non-linear internal wave phenomena, in analogy to the progress that has been made in understanding nonlinear mountain flows[1] (Smith, 1979; Wurtele et al., 1996). DNS enables the investigation of numerical and parametric sensitivities of internal wave processes. This enhances our understanding of similar processes in climate and weather prediction models, where the distinction between numerically gen-

[1] It should be noted, that in contrast to the classical formulation of the lee wave problem (Wurtele et al., 1996), phenomena like the quasi-biennial oscillation (QBO) entail self-induced variable background states.

erated and "real" effects is less obvious. Global observations of internal wave processes in the atmosphere are just emerging but their distinction from the medium in which they propagate as well as the determination of their spatial and temporal distribution, due to their transient character, is difficult (Alexander and Holton, 2004). High resolution global atmospheric models may be used to compensate for the lack of global observations of internal waves, since they resolve part of the internal wave spectrum. However, the numerical realization of waves may be strongly influenced by the choice of the numerical methods used, the discretisation, the choice and the numerical implementation of upper and lower boundary conditions, and simplifications as well as sub-grid scale parametrizations of the gravity wave sources, i.e. convection and topography.

A new numerical framework described in detail in Wedi and Smolarkiewicz (2004a) has been developed to simulate weakly-stratified fluids while adapting to complicated time-dependent boundaries. In particular, it has been applied in the direct numerical simulation of the laboratory analogue of the quasi-biennial oscillation (QBO), the dominant variability in the equatorial stratosphere (Baldwin et al., 2001). The QBO analogue exhibits a number of internal gravity wave processes, wave reflection, wave interference, wave-mean flow interaction, critical layer formation and subsequent wave breaking, all of which are found in the atmosphere. In contrast to atmospheric modelling studies, the forcing wave spectrum is explicitly known and in contrast to laboratory experiments far more information is available for process identification. It is therefore that the use of this numerical framework in the context of DNS becomes a useful tool as a confined numerical "laboratory" environment to study internal waves and their numerical realisability (Wedi, 2004; Wedi and Smolarkiewicz, 2004b).

2 The laboratory analogue of the QBO and its numerical equivalent

The quasi-biennial oscillation (QBO) exhibits a fundamental dynamical mechanism with challenging detail. Lindzen and Holton (1968) and Holton and Lindzen (1972) were among the first to present a conceptual model of the QBO describing the oscillation as an interaction between the mean flow and propagating waves. In a viscous, non-rotating Boussinesq fluid, the interaction can be described by the averaged momentum equations in a horizontally periodic domain as

$$\frac{\partial U}{\partial t} - \nu \frac{\partial^2 U}{\partial z^2} = -\sum_i \frac{\partial F_i}{\partial z}, \tag{1}$$

where $U := \overline{u}^{xy}$ denotes the horizontally averaged (mean) flow, ν denotes the kinematic viscosity and $F := \overline{u'w'}^{xy}$ expresses the averaged nonlinear momentum flux.[2] Most atmospheric research of the QBO is devoted to finding the precise origins of the rhs of equation (1) and their numerical realisability in the context of numerical weather prediction and climate models. In spite of numerous studies, see Baldwin et al. (2001) for a recent review, a complete understanding of the QBO eludes the efforts.

The principal mechanism of the QBO was demonstrated in the laboratory experiment of Plumb and McEwan (1978). The laboratory analogue of the stratospheric equatorial oscillation consists of a cylindrical annulus filled with density-stratified salty water, forced at the lower boundary by an oscillating membrane. At sufficiently large forcing amplitude the wave motion generates a longer period zonal mean flow oscillation. The laboratory experiment is often employed to explain the basic mechanism of the atmospheric QBO (Baldwin et al., 2001).

The equations of motion for a non-rotating, density-stratified viscous Boussinesq fluid — an appropriate ap-

[2] In the context of time-varying mean flow oscillations it is important to note that the second "Eliassen-Palm theorem" (Eliassen and Palm, 1961), stating the height independence of the vertical flux of horizontal momentum $\overline{u'w'}^{xy}$, refers to a steady state in the absence of damping and critical levels.

proximation for salty water Gill (1982) — are:

$$\begin{aligned} \nabla\cdot\left(\rho_0\mathbf{v}\right) &= 0\,, \\ \frac{D\mathbf{v}}{Dt} &= -\nabla\pi' + \mathbf{g}\frac{\rho'}{\rho_0} + \frac{1}{\rho_0}\nabla\cdot\tau\,, \\ \frac{D\rho'}{Dt} &= \kappa\nabla^2\rho' - \mathbf{v}\cdot\nabla\rho_e\,. \end{aligned} \tag{2}$$

Here, the operators D/Dt, ∇, and $\nabla\cdot$ symbolise the material derivative, gradient, and divergence; $\mathbf{v}$ denotes the velocity vector; ρ' and π' denote, respectively, density and normalised-pressure perturbations with respect to the static ambient state characterised by the linearly stratified profile ρ_e; $\mathbf{g}$ symbolises the gravity vector, and ρ_0 a constant reference density. $\nabla\cdot\tau$ is the divergence of the viscous stress tensor ($\tau_{ij}\sim\nu$) with ν ($=1.004\times10^{-6}m^2s^{-1}$) the kinematic viscosity; and κ ($=1.5\times10^{-9}m^2s^{-1}$) is the diffusivity of salt in water.

The equations (2) are cast in a time-dependent curvilinear framework (Prusa and Smolarkiewicz, 2003; Smolarkiewicz and Prusa, 2004), employing the generalised Gal-Chen coordinate transformation

$$\bar{t}=t,\quad \bar{x}=x,\quad \bar{y}=y,\quad \bar{z}=H_0\frac{z-z_s(x,y,t)}{H(x,y,t)-z_s(x,y,t)}\,, \tag{3}$$

whose theoretical development and efficient numerical implementation were discussed thoroughly in Wedi and Smolarkiewicz (2004a). The transformation (3) allows for time-dependent upper and lower boundary forcings without small-amplitude approximations. In particular, it enables the direct numerical simulation of the laboratory experiment. In standard atmospheric models a major uncertainty arises from the lack of knowledge of the required wave forcing and its numerical realisability, rendering a detailed analysis of the QBO more difficult.

The governing equations (2) are integrated numerically in the transformed space using a second-order-accurate, optionally semi-Lagrangian or Eulerian, nonoscillatory forward-in-time (NFT) approach, broadly documented in the literature (cf. Smolarkiewicz and Prusa (2004) for a brief summary). Both algorithms, flux-form Eulerian or semi-Lagrangian, are based on the monotone MPDATA transport scheme (Smolarkiewicz and Margolin, 1998). All prognostic equations in (2) are integrated along flow trajectories using the trapezoidal rule, treating all forcings on the rhs implicitly; the viscous and diffusive terms are computed to first-order accuracy, assuming $\nabla\cdot\tau^{n+1}=\nabla\cdot\tau^n+\mathscr{O}(\Delta t)$ (and similar for $\kappa\nabla^2\rho'$); see section 3.5.4 in Smolarkiewicz and Margolin (1998). Together with the curvilinearity of the coordinates, this leads to a complicated elliptic problem for pressure (see Appendix A in Prusa and Smolarkiewicz (2003) for the complete description) solved iteratively using the preconditioned generalised conjugate-residual approach — a nonsymmetric Krylov-subspace solver (Smolarkiewicz and Margolin, 2000).

The numerical setup of the DNS and preliminary results are summarised in Wedi and Smolarkiewicz (2004b) and a detailed account of the simulations is given in Wedi (2004). A schematic description of a typical sequence of events is given in figure 1. A single horizontal wave number and a range of vertical wave numbers are observed. The internal waves interfere with each other in the vertical, causing spatial background flow perturbations that result in wave momentum flux changes, which in return contribute to a change in the background flow. This background flow grows to the extent that it becomes nearly as large as the horizontal propagation speed of the forcing waves, i.e. a critical layer forms (asymptotically a critical level as in Booker and Bretherton, 1967)). At this point the critical shear layer continues to grow downward towards the forcing membrane, due to enhanced dissipation by wave breaking, which is observed within the critical layer. When it arrives at the membrane, it forces waves propagating in the opposite direction and the mechanism repeats with reversed signs.

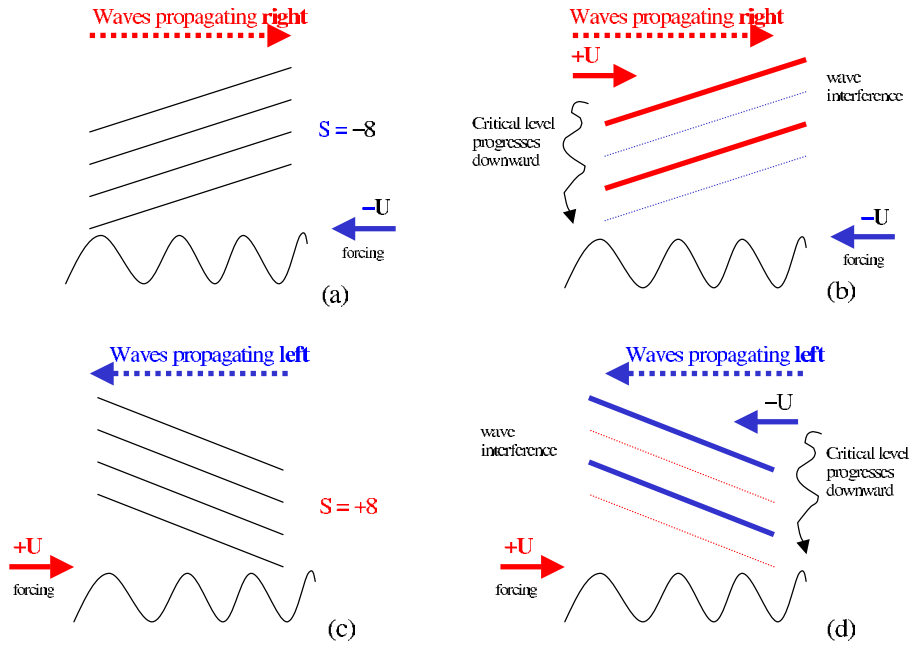

Figure 1: The principle mechanism of the oscillation in the laboratory experiment of Plumb and McEwan is shown in 4 representative phases of the mean flow.

3 Numerical sensitivities of zonal mean flow oscillations

In this section some aspects of numerical realisability are investigated where the onset of the zonal mean flow oscillation and the length of its period are used as a measure of numerical error.

It is found that initially an asymmetric excitation is required to start the oscillation. This may be as small as asymmetrically accumulated numerical round-off errors, as found when there was a bug in the parallelisation, which created a continuous but tiny asymmetry in the zonal periodicity. Without initial noise or other asymmetry the 3D simulation with a forcing amplitude equivalent to the laboratory setup failed to initiate an oscillation. However, in a simulation with twice that forcing amplitude, an asymmetry develops quickly and a zonal mean flow oscillation starts. It is speculated that in the latter case the increased nonlinearity (turbulence) induces either a numerically enforced asymmetry or an inherent asymmetry of the nonlinear terms. In any case, it indicates that a small excitation suffices, whether resulting from the inherent nonlinearity or from an external source.

The onset of the zonal mean flow oscillation was also dependent on different numerical approximations. Substantial variations in the onset of the oscillation are found for example with first order accurate advection which starts an oscillation almost immediately, albeit an unrealistic period and time evolution. Variations in the onset were also found between semi-Lagrangian and flux-form Eulerian advection.

Numerical sensitivities with respect to the period are found in particular when using more diffusive numerical methods. Increased implicit diffusion results in shorter periods. The same is true for the comparison between the flux-form Eulerian compared to the semi-Lagrangian approach (see Smolarkiewicz and Margolin (1993) and Smolarkiewicz and Pudykiewicz (1992) for details of the implementation), where the semi-Lagrangian advection produces a marked shorter and irregular period (see figure2). This is also reflected in the comparison of the energy budgets of the simulations where the semi-Lagrangian method exhibits an unphysical growth of potential energy in contrast to the flux-form Eulerian approach. The results agree with the findings in Smolarkiewicz and Margolin (1997) where a flux-form Eulerian formulation, with a small viscosity explicitly added, gave closer agreement with the corresponding semi-Lagrangian simulation. Since in general flux-form schemes have higher-order truncation errors proportional to the differentials of fluxes of the primitive variables

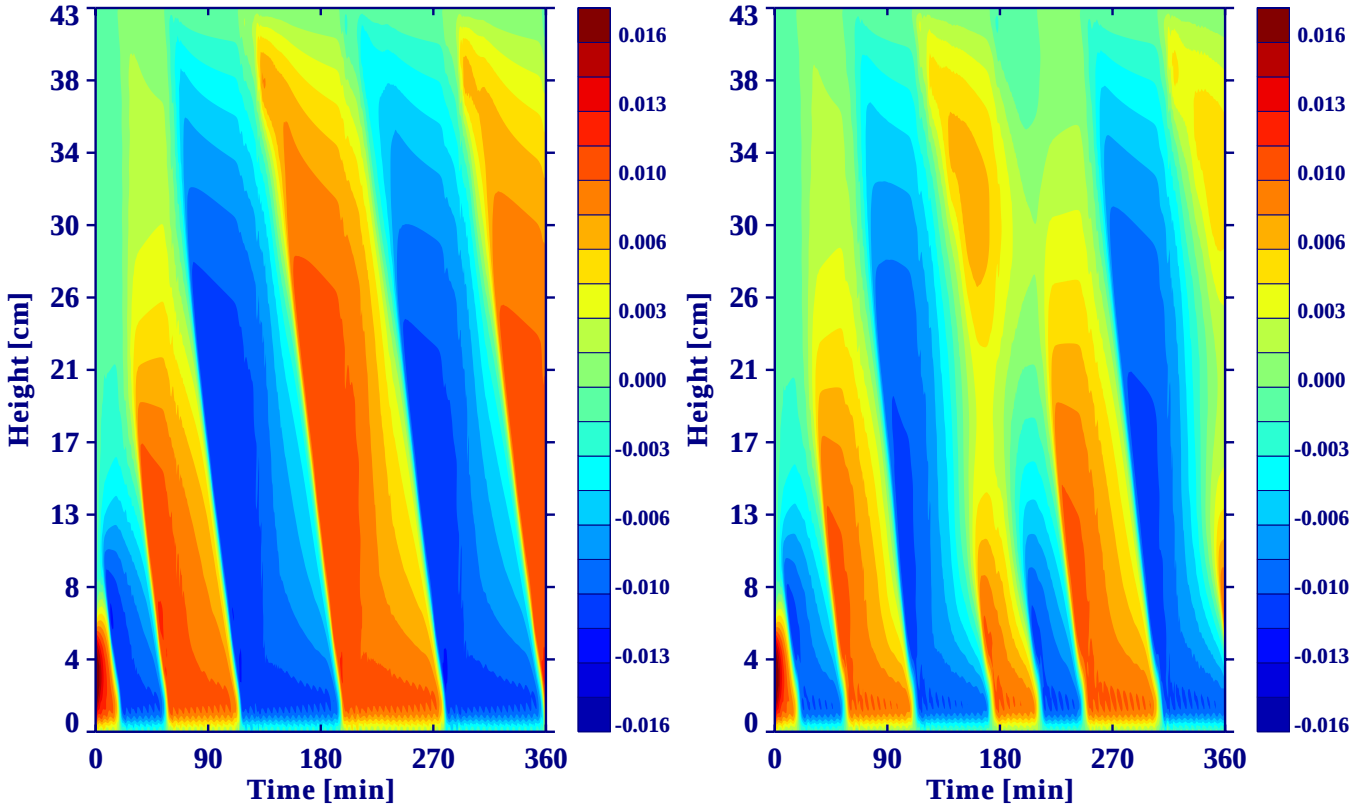

Figure 2: Time-height cross-section of the zonal-mean flow velocity in the 2D numerical simulation using a noslip rigid upper boundary a) with a flux-form Eulerian advection scheme and b) with a semi-Lagrangian advection scheme. The phases are noticeably distorted in the semi-Lagrangian case, which is also found to conserve energy less accurately.

rather than to the differentials of the variables themselves (as characteristic of advective form schemes), they concluded that the overall accuracy of the approximation increases when the fluxes of the variables exhibit a greater degree of homogeneity than the variables themselves (Smolarkiewicz and Margolin, 1997). This appears to be the case in the QBO analogue simulations with fairly steady wave momentum fluxes below the critical layer.

The results were not very sensitive to the chosen numerical accuracy of the pressure solver. However, when the accuracy is reduced to $\|\Delta t \nabla \cdot \mathbf{v}\| < \varepsilon = 10^{-3}$ (see Smolarkiewicz et al. (1997) for a discussion) and only a single iteration is enforced to obtain convergence, the period of the mean flow oscillation distorts and becomes much larger than in the reference solution. Also an explicit vs. implicit solution procedure with respect to the internal gravity waves has been analysed. In the explicit case full ρ is advected whereas in the implicit case only the perturbation ρ'. This influences the numerical solution procedure in the implicit case due to the appearance of the convective derivative in the thermodynamic equation. Here, this equation has to be solved simultaneously with the momentum equation (see the appendix in Smolarkiewicz et al. (2001) for details). The same time-step was used for both integrations. The explicit solution gives only a weak and distorted oscillation period similar to the lower accuracy solution above. Notably, doubling the vertical resolution in the explicit case almost recovers the implicit solution. From the comparison of the waves generated in both solutions it is concluded that the dispersion of the waves is little effected by the implicit calculations but the explicit solution procedure is inferior in accuracy.

It is evident that sufficient resolution is required in particular in the vertical to resolve the initiating internal gravity waves, otherwise no zonal mean flow oscillation is observed. This necessitates of course the knowledge of the waves, responsible for the generation of the stratospheric equatorial QBO. Resolution changes appear to impact mainly the speed of the apparent downward propagation which may relate to a better representation of the ratio of dynamic and viscous scales. Increasing horizontal and vertical resolutions increases the period up to 20-30% in the simulations up to a 'saturation threshold' after which the mean flow oscillation period is more less invariant to resolution change. All simulations shown here have been conducted with resolutions in excess of this 'saturation threshold'.

In two dimensions, the boundary conditions influencing wave reflection can alter the period substantially depending on the geometry of the domain and the propagation speed of the contributing internal gravity waves. For simulating non-reflecting boundary conditions it has been found beneficial to apply the absorber only on zonal wind but not on density perturbations, providing least impact on the interior domain. In three dimensions the upper boundary had negligible influence due the viscosity of the water and due to the amplitude decay of three-dimensional gravity waves, unlike two-dimensional hydrostatic flow (Smith, 1980). However, in non-Boussinesq simulations the amplitude growth of vertically propagating waves, due the the decrease of density with height, offsets this decay and may raise again the importance of upper boundary influences.

4 Zonal mean flow oscillations in global circulation models

There have been a number of 2D mechanistic models (based on the horizontally averaged momentum equations) successful in simulating a QBO-like oscillation but 3D modelling of the QBO has largely been unsuccessful. The reasons are not entirely clear. Nevertheless, QBO-like oscillations in 3D have recently been successfully modelled by (Takahashi, 1999; Giorgetta et al., 2002; Untch, 1998). It appears from these studies, that a successful model of the atmospheric QBO requires sufficient vertical resolution, some "tuning" with respect to horizontal and vertical diffusion parameters and in particular a parametrization or other means to produce a sufficiently broad spectrum of vertically propagating gravity waves. The ECMWF model has apparently lost its ability to successfully model a QBO-like oscillation (Untch, 1998) despite various efforts to find the cause of this change and despite recent resolution enhancements and considerable progress in forecast ability (Simmons and Hollingsworth, 2002).

Sufficient vertical resolution has been found necessary Giorgetta et al. (2002), but above all vertically propagating gravity waves are required in the stratosphere with sufficient amplitude (energy) to produce mean flow changes. The most effective way to create those waves in the ECMWF model is by switching off the convective parametrization (P.Bechtold, personal communication). Lacking diabatic convective forcing to compensate the adiabatic tendencies, the model produces strong localised convergence patterns (figure4) at the grid-scale, which in return produce large amplitude, vertically propagating gravity waves. It is those waves that suffice to produce (again) a QBO-like oscillation in a climate integration using the latest forecast model at ECMWF (figure 3 and 4).

The apparently paradoxical explanation for the inability to model a QBO-like oscillation in the past years may therefore be given as the result of recent improvements in the convection scheme aimed at avoiding numerically generated gridscale divergences. A comparison with the magnitude of gravity waves resulting from the operational convection scheme (Tiedke, 1989) shows indeed a large difference in the amplitudes of the generated waves. Furthermore, since horizontal diffusion primarily acts on the tail of the spectrum of the resolved gravity waves in global atmospheric models, the "tuning" of horizontal diffusion, which helped to obtain a QBO-like oscillation in Takahashi (1999), is readily understood as varying the degree of suppression of gravity wave forcing. These QBO simulations may therefore serve as an indication that a seemingly correct physical response may be obtained for numerical reasons only. Furthermore, there is an open question how the effect of resolved wave breaking is simulated in hydrostatic models like IFS, while invalidating the underlying equations. Typically nearly vertical steepening of isentropic surfaces is found (see e.g. Wedi and Smolarkiewicz (2004a) for

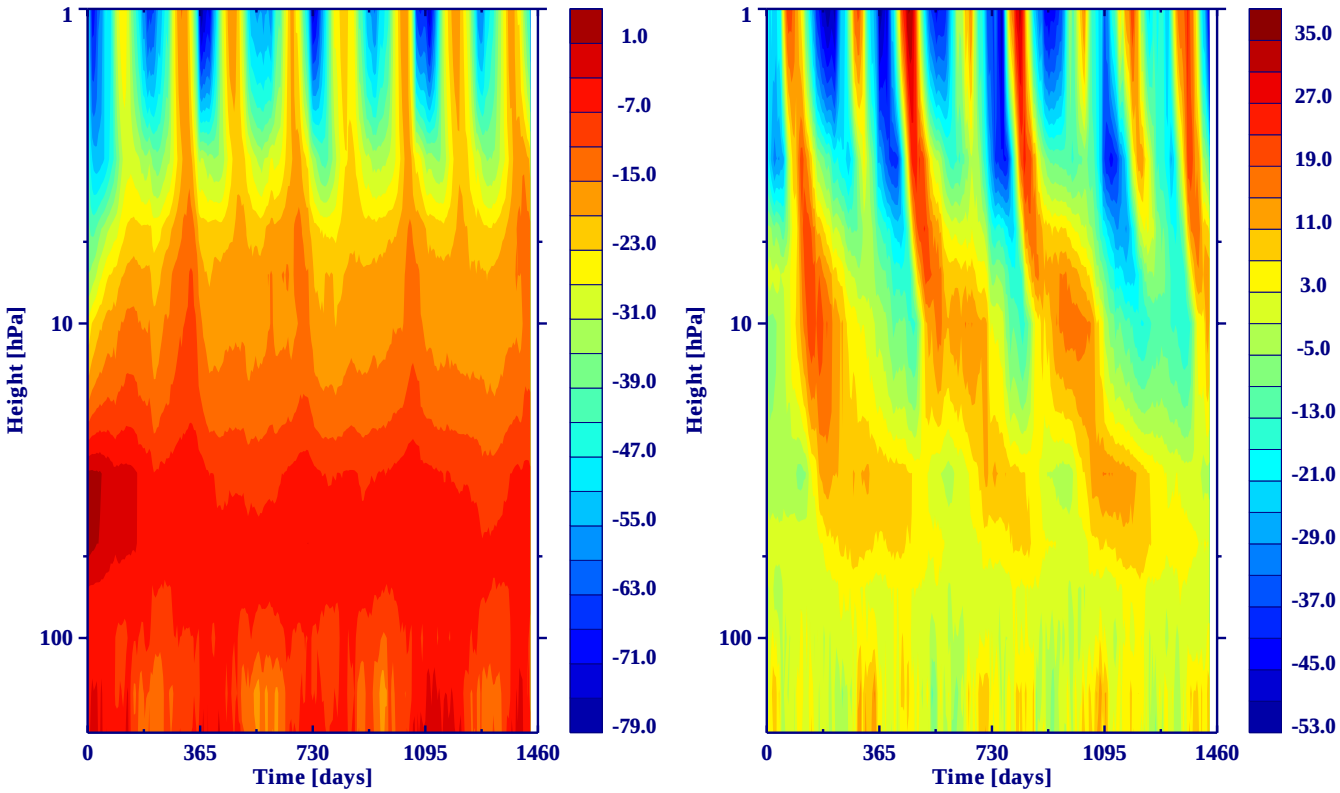

Figure 3: A QBO-like oscillation in a T63 IFS model simulation with 91 levels and no parametrized convection in the simulation. The left plate shows the time height cross-section at the equator for the experiment using the Tiedke convection scheme and the right plate shows the case with the convection scheme switched off.

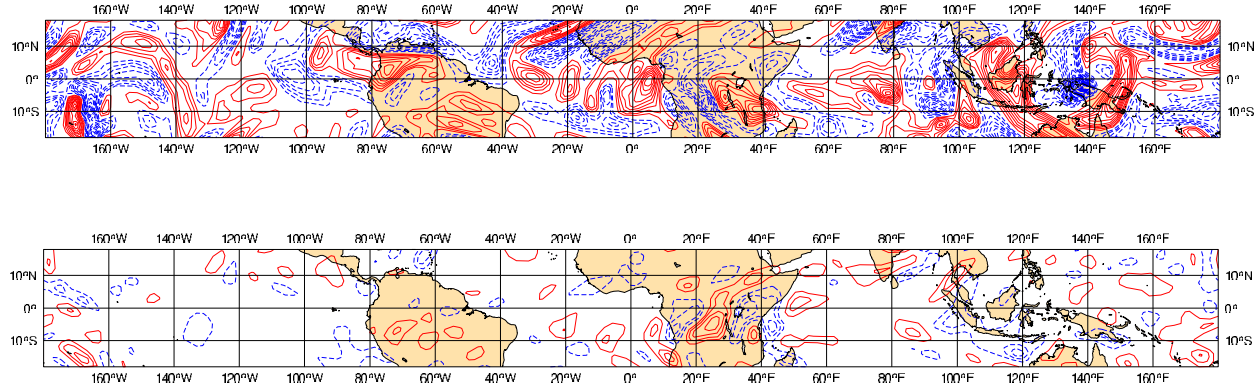

Figure 4: Instantaneous horizontal distribution of the driving forces for the QBO-like oscillation in the T63 IFS model with 91 levels. The simulation develops some strong local events throughout the troposphere reaching as high as model level 39 ($\approx 100hPa$), which is shown here. The figures show horizontal velocity divergence. Strong divergences on the grid-scale can be identified that develop in the simulation without parametrized convection; the bottom figure exhibits the relative lack of such events when using the Tiedke massflux convection scheme. The contour interval is $0.5s^{-1}$ in both plates.

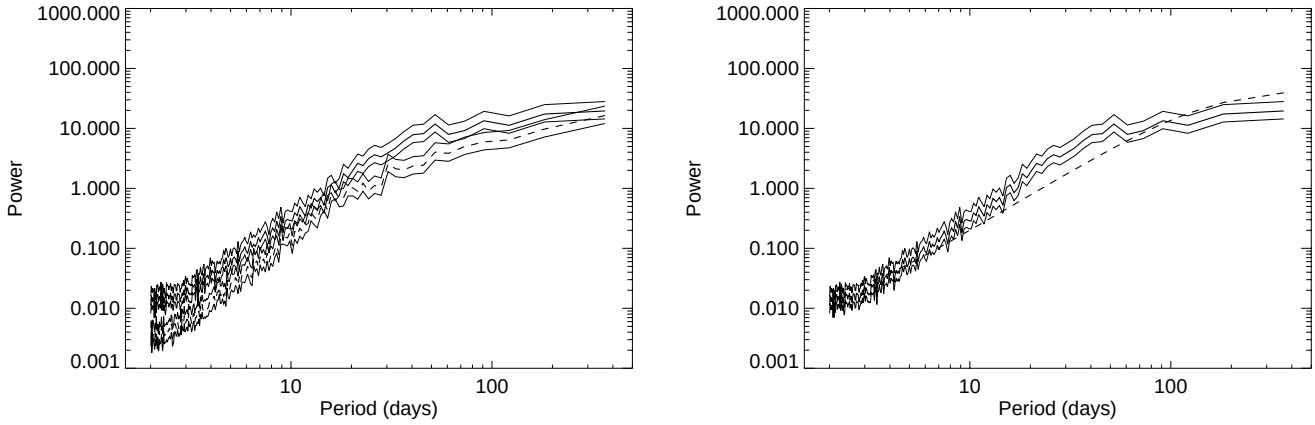

Figure 5: Power spectra of the zonal mean zonal velocity component at 500 hPa averaged between -10 *and* $+10$ *degrees latitude over 35 years. The left plate compares the ERA40 analysis with a corresponding* T_l159 *climate simulation of the same length. The solid line denotes the ERA40 analysis spectrum. he dashed line denotes the* T_l159 *climate simulation. The corresponding 95 % confident intervals around the spectra are also shown. The right plate compares the ERA40 analysis data (solid line) with a "red noise" spectrum (dashed line), modelled by a first order autoregressive (AR(1)) process. It shows that the variability in the time series in the range* $20-60$ *days is inconsistent with a purely stochastic red noise process, which represents the null hypothesis of no statistically significant oscillations (von Storch and Zwiers, 1999).*

an analogy of a hydraulic jump with an approximated shallow water surface). While the waves may not break in a physical sense there is still a contribution from the resolved waves to the nonlinear products of velocity components in the rhs of equation (1). Giorgetta et al. (2002) found approximately equal contributions to the wave momentum fluxes of resolved and parametrized internal gravity waves in their successful simulation of a QBO-like oscillation.

The zonal mean flow oscillation discussed so far has been generated by wave-induced vertical transport of momentum. However, in the troposphere there are a number of waves which may similarly interact to create zonal mean flow oscillations resulting from meridional variations in which case the governing zonally averaged momentum equation results as

$$\frac{\partial U}{\partial t} = -\frac{\partial}{\partial y} < u'v' >_x . \tag{4}$$

Such mean flow oscillations due to wave interference (in the absence of wave dissipation) are only possible for the same or opposite zonal wavenumber in agreement with (Lindzen et al., 1982) who already noted the possibility of such horizontal vacillations in the atmosphere. The term on the right hand side of equation (4) is reminiscent of the term in (Moncrieff, 2004) formulating a forcing relation for the Madden-Julian oscillation (MJO) (Madden and Julian, 1972, 1994) which represents the major observed mode in the tropical troposphere and which is neither well understood nor accurately modelled in three-dimensional forecast or climate models. Figure 5 presents evidence of an equatorial zonal mean flow oscillation signal with a broad period of 20-60 days in the ERA40 re-analysis data and has also been observed in other variables (see (Madden and Julian, 1994) for a review). The signal is absent from the corresponding T_l159 climate simulation (Simmons et al., 2004). However, a four month long, high resolution T_l511 climate simulation exhibits a similar periodicity in the zonally averaged zonal velocity component, where internal wave interactions may provide an explanation.

5 Discussion

There is a long list of numerical influences on internal (gravity) wave dispersion and dissipation, and their distinction from physical phenomena may not always be obvious. Current and future high resolution global circulation models resolve part of these internal wave processes but may not be accurate. If tropospheric wave interactions are found to have an influence on medium range predictability, as suggested by the otherwise unexplained MJO signal in the zonal mean zonal velocity component, this may pose new demands on dynamical core test cases beyond Held-Suarez type simulations. For climate simulations, it further stresses the need for appropriate parametrizations, expressing the statistical effects of internal wave dissipation and wave interactions (see Kim et al. (2003) for a review). The precise specification of a variety of gravity wave forcings in the numerical framework described in Wedi (2004) together with the accurate simulation of internal gravity wave dynamics would represent an appropriate testbed for these parametrizations. Furthermore, the theory and the numerical apparatus may well be extended to provide a "laboratory" analogue for the MJO.

Acknowledgements

First of all I would like to thank Piotr Smolarkiewicz for his constant support and invaluable supervision of this work. I would like to thank Antony Hollingsworth for the stimulating suggestion to apply the numerical framework to the QBO analogue. Tim Palmer is thanked for providing the VHS movie of the original laboratory experiment. I would also like to thank especially Agathe Untch and Mariano Hortal for numerous discussions and reviews. I am grateful to Martin Miller for his support and for reviewing the manuscript. I would like to express a special thanks to Adrian Tompkins for his help with IDL, Thomas Jung for providing the MJO power spectra, Peter Bechtold for suggesting to switch off convection and IBM for allowing me to use sufficient time on the familiarisation test-cluster for the simulations.

References

Alexander, M. and J. Holton (2004). On the spectrum of vertically propagating gravity waves generated by a transient heat source. *Atmos. Chem. Phys. 4*, 923–932.

Baines, P. (1995). *Topographic effects in stratified flows*. Cambridge, New York: Cambridge University Press.

Baldwin, M., L.J., T. Dunkerton, K. Hamilton, P. Haynes, W. Randel, J. Holton, M. Alexander, I. Hirota, T. Horinouchi, D. Jones, J. Kinnersley, C. Marquardt, K. Sato, and M. Takahashi (2001). The quasi-biennial oscillation. *Reviews Geophys. 39*(2), 179–229.

Booker, J. and F. Bretherton (1967). The critical layer for internal gravity waves in a shear flow. *J. Fluid Mech. 27*, 513–539.

Bretherton, F. (1966). The propagation of groups of internal gravity waves in a shear flow. *Q.J.R. Meteorol. Soc. 92*, 466–480.

Daley, R. (1988). The normal modes of the spherical non-hydrostatic equations with applications to the filtering of acoustic modes. *Tellus 40A*, 96–106.

Eliassen, A. and E. Palm (1961). On the transfer of energy in stationary mountain waves. *Geofys. Publ. 22*, 1–23.

Fritts, D. and M. Alexander (2003). Gravity wave dynamics and effects in the middle atmosphere. *Reviews Geophys. 41*, 1–68.

Galmiche, M., O. Thual, and P. Bonneton (2000). Wave/wave interaction producing horizontal mean flows in stably stratified fluids. *Dyn. Atm. Ocean 31*, 193–207.

Gill, A. (1982). *Atmosphere-Ocean Dynamics*, Volume 30 of *International geophysics series*. London: Academic Press.

Giorgetta, M., E. Manzini, and E. Roeckner (2002). Forcing of the quasi-biennial oscillation from a broad spectrum of atmospheric waves. *Geophys. Res. Lett. 29*(8), 86–1–86–4.

Grimshaw, R. (1972). Nonlinear internal gravity waves in a slowly varying medium. *J. Fluid Mech. 54*, 193–207.

Grimshaw, R. (1974). Internal gravity waves in a slowly varying dissipative medium. *Geophys. Fluid Dyn. 6*, 131–148.

Grimshaw, R. (1975). Nonlinear internal gravity waves and their interaction with the mean wind. *J. Atmos. Sci. 32*, 1779–1793.

Holton, J. and R. Lindzen (1972). An updated theory for the quasi-biennial cycle of the tropical stratosphere. *J. Atmos. Sci. 29*, 1076–1079.

Kasahara, A. and J.-H. Qian (2000). Normal modes of a global nonhydrostatic model. *Mon. Weather Rev. 128*, 3357–3375.

Kim, Y.-J., D. Eckermann, and H.-Y. Chun (2003). An overview of the past, present and future of gravity-wave drag parameterization for numerical climate and weather prediction models. *Dyn. Atm. Ocean 41*, 65–98.

Koop, C. (1981). A preliminary investigation of the interaction of internal gravity waves with a steady shearing motion. *J. Fluid Mech. 113*, 347–386.

Koop, C. and B. McGee (1986). A preliminary investigation of the interaction of internal gravity waves with a steady shearing motion. *J. Fluid Mech. 172*, 453–480.

Lindzen, R., B. Farrell, and D. Jacqmin (1982). Vacillations due to wave interference: Applications to the atmosphere and to annulus experiments. *J. Atmos. Sci. 39*, 14–23.

Lindzen, R. and J. Holton (1968). A theory of the quasi-biennial oscillation. *J. Atmos. Sci. 25*, 1095–1107.

Madden, R. and P. Julian (1972). Description of global scale circulation cells in the tropics with 40-50 day period. *J. Atmos. Sci. 29*, 1109–1123.

Madden, R. and P. Julian (1994). Observations of the 40-50-day tropical oscillation - a review. *Mon. Weather Rev. 122*, 814–837.

Moncrieff, M. (2004). Analytic representation of the large scale organization of tropical convection. *J. Atmos. Sci.*. in press.

Phillips, N. (1981). Wave interactions - the evolution of an idea. *J. Fluid Mech. 106*, 215–227.

Phillips, N. (1990). Dispersion in large scale weather prediction. *WMO Sixth IMO lecture*.

Plumb, R. and D. McEwan (1978). The instability of a forced standing wave in a viscous stratified fluid: A laboratory analogue of the quasi-biennial oscillation. *J. Atmos. Sci. 35*, 1827–1839.

Prusa, J. and P. Smolarkiewicz (2003). An all-scale anelastic model for geophysical flows: dynamic grid deformation. *J. Comput. Phys. 190*, 601–622.

Simmons, A. and A. Hollingsworth (2002). Some aspects of the improvement in skill of numerical weather prediction. *Q.J.R. Meteorol. Soc. 128*, 647–677.

Simmons, A., P. Jones, V. da Costa Bechtold, A. Beljaars, P. Kallberg, S. Saarinen, S. Uppala, P. Viterbo, and N. Wedi (2004). Comparison of trends and variability in cru, era40 and ncep/ncar analysis of monthly-mean surface air temperature. *J. Geophys. Res.*. submitted.

Smith, R. (1979). The influence of mountains on the atmosphere. *Adv. Geophys. 21*, 87–230.

Smith, R. (1980). Linear theory of stratified hydrostatic flow past an isolated mountain. *Tellus 32*, 348–364.

Smolarkiewicz, P., V. Grubišić, and L. Margolin (1997). On forward-in-time differencing for fluids: Stopping criteria for iterative solutions of anelastic pressure equations. *Mon. Weather Rev. 125*, 647–654.

Smolarkiewicz, P. and L. Margolin (1993). On forward-in-time differencing for fluids: Extension to a curvilinear framework. *Mon. Weather Rev. 121*, 1847–1859.

Smolarkiewicz, P. and L. Margolin (1997). On forward-in-time differencing for fluids: An Eulerian/semi-Lagrangian non-hydrostatic model for stratified flows. *Atmos. Ocean Special 35*, 127–152.

Smolarkiewicz, P. and L. Margolin (1998). Mpdata: A finite difference solver for geophysical flows. *J. Comput. Phys. 140*, 459–480.

Smolarkiewicz, P. and L. Margolin (2000). Variational methods for elliptic problems in fluid models. In *Proc. ECMWF Workshop on Developments in numerical methods for very high resolution global models*, Reading, UK, pp. 137–159. Eur. Cent. For Medium-Range Weather Forecasts.

Smolarkiewicz, P., L. Margolin, and A. Wyszogrodzki (2001). A class of nonhydrostatic global models. *J. Atmos. Sci. 58*, 349–364.

Smolarkiewicz, P. and J. Prusa (2004). Toward mesh adaptivity for geophysical turbulence. *Int. J. Numer. Methods Fluids*. to appear.

Smolarkiewicz, P. and J. Pudykiewicz (1992). A class of semi-Lagrangian approximations for fluids. *J. Atmos. Sci. 49*, 2082–2096.

Staquet, C. and J. Sommeria (2002). Internal gravity waves: from instabilities to turbulence. *Annu. Rev. Fluid Mech. 34*, 559–593.

Takahashi, M. (1999). Simulation of the quasi-biennial oscillation in a general circulation model. *Geophys. Res. Lett. 26*(9), 1307–1310.

Thuburn, J., N. Wood, and A. Staniforth (2001). Normal modes of deep atmospheres I: spherical geometry. *Q.J.R. Meteorol. Soc. 128*, 1771–1792.

Tiedke, M. (1989). A comprehensive mass flux scheme for cumulus parameterization. *Mon. Weather Rev. 117*, 1779–1800.

Untch, A. (1998). Aspects of stratospheric modelling at ECMWF. In *Proc. ECMWF Workshop on Recent Developments in numerical methods for atmospheric modelling*, Reading, UK, pp. 442–453. Eur. Cent. For Medium-Range Weather Forecasts.

von Storch, H. and F. Zwiers (1999). *Statistical Analysis in Climate Research*. Cambridge University Press.

Wedi, N. (2004). *Time-dependent boundaries in numerical models*. Ph. D. thesis, Ludwig-Maximilians-Universität München, Institut für Physisk der Atmosphäre des DLR, Oberpfaffenhofen. submitted.

Wedi, N. and P. Smolarkiewicz (2004a). Extending Gal-Chen & Somerville terrain-following coordinate transformation on time-dependent curvilinear boundaries. *J. Comput. Phys. 193*, 1–20.

Wedi, N. and P. Smolarkiewicz (2004b). Laboratory for internal gravity-wave dynamics: The numerical equivalent to the quasi-biennial oscillation (QBO) analogue. *Int. J. Numer. Methods Fluids*. submitted.

Wurtele, M., R. Sharman, and A. Datta (1996). Atmospheric lee waves. *Annu. Rev. Fluid Mech. 28*, 429–476.